Materials Advances

ROYAL SOCIETY OF CHEMISTRY

REVIEW

View Article Online
View Journal | View Issue

Cite this: *Mater. Adv.*, 2021, 2, 2510

Recent advances in mechanochemical synthesis of mesoporous metal oxides

Barbara Szczęśniak, [a] Jerzy Choma [a] and Mietek Jaroniec *[b]

Received 27th January 2021,
Accepted 9th March 2021

DOI: 10.1039/d1ma00073j

rsc.li/materials-advances

There is growing interest in mesoporous metal oxides due to their unique properties such as highly accessible porosity, stability, catalytic activity and diversity of nanostructures. Mechanochemical fabrication of mesoporous metal oxides is gaining increasing attention because it can be a promising alternative to conventional solvent-based syntheses, which are often complex, and time- and energy consuming. A large variety of mesoporous metal oxides have been already prepared by means of mechanochemistry, and we believe that there is a need to summarize recent achievements in this research area. This review covers recent advances and challenges in the synthesis of mesoporous metal oxides and related materials with special emphasis on mechanochemically obtained mesostructures.

1. Introduction

Mesoporous materials have been synthesized in the early 1990s, *e.g.*, Kuroda *et al.*[1] used alkyltrimethylammonium ions with varying alkyl chain length to expand interlayer spaces in polysilicates up to 4 nm. A real breakthrough in the area of mesoporous materials was reported in 1992 by showing a simple and effective way for synthesizing ordered mesoporous silicas *via* self-assembly of silica species and cationic surfactants.[2,3] Since this discovery, extensive efforts have been made toward the synthesis of ordered mesoporous materials (OMMs) including silicas, organosilicas, metal oxides, carbons, zeolites, metal– and covalent–organic frameworks and almost countless two- or three-component composites based on these OMMs.[4] Major developments in the field of OMMs are presented in Fig. 1.

The driving force for synthesizing porous oxides with ordered and/or uniform mesopores is the need for improving their catalytic/adsorption properties. For instance, ordered mesoporous channels in solids improve mass transfer and diffusion as well as expose active sites.[5] Moreover, they enhance the accessibility of the entire surface area for adsorption of various ions and molecules. Mesoporous metal oxides have already shown great performance in various catalytic processes because of their large pore sizes and high pore volume.[6–8] Thus, they attract a lot of attention and are designed for real applications. The ability to precisely control the pore size of nanomaterials is important to meet special requirements for specific hi-tech applications.

Nowadays, mesopores in solids are commonly created by using templating strategies.[4,9–13] Hard templating involves the use of rigid templates (*e.g.*, mesoporous silica, colloidal crystals, and spherical nanoparticles), which need to be removed at the final step of the synthesis usually *via* dissolution with HF or NaOH solutions. This strategy is convenient and enables a large variety of mesoporous solids to be obtained, but it is time consuming, expensive and requires specific templates. Moreover, to obtain the reverse replicas of templates the precursors used need to homogenously fill the template pores. Soft templating methods are more straightforward. They rely on the ability of surfactants or block copolymers to assemble into micellar mesostructures and can be removed more easily either by thermal decomposition or extraction. In this case, the precursors having small enough sizes should be able to interact and assemble around the template micelles.[14] The salt templating strategy has emerged recently as an alternative to the classical soft and hard templating methods. Although the templates used in salt templating are usually cheap and can be removed easily even by washing with water, the created mesopores are not uniform. Thus, it is very difficult to control/tune the porosity in the resulting materials.

There are numerous reviews devoted to OMMs including mesoporous metal oxides,[4,7,8] *e.g.*, our previous review providing an overview of all major groups of OMMs.[4] However, this field is continuously growing. In particular, mechanochemical synthesis of mesoporous metal oxides seems to be an emerging area with many potential applications of the resulting materials. Therefore, we believe that a concise presentation of recent advancements in this field would be desirable and may encourage researchers to find the mechanochemical method to be an attractive option in the synthesis. In this review a special emphasis is given to the mechanochemical synthesis of various metal oxides because at

[a] *Institute of Chemistry, Military University of Technology, 00-908 Warsaw, Poland. E-mail: barbara.szczesniak@wat.edu.pl, jerzy.choma@wat.edu.pl*
[b] *Department of Chemistry and Biochemistry & Advanced Materials and Liquid Crystal Institute, Kent State University, Kent, Ohio 44242, USA. E-mail: jaroniec@kent.edu; Fax: 330-672-3816; Tel: 330-672-3790*

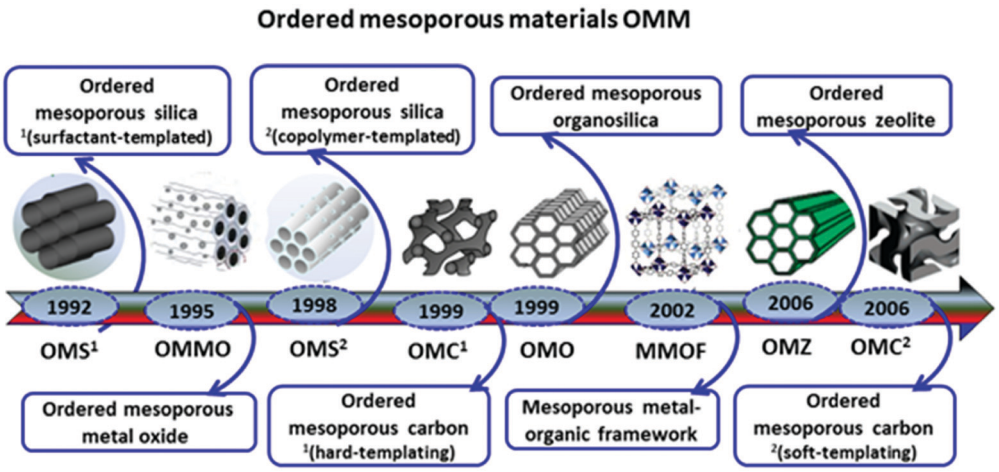

Fig. 1 Schematic illustration of major developments in the synthesis of OMMs.[4]

the current stage it is still challenging to prepare sustainable materials with uniform mesopores and high crystallinity. This review also presents the evolution of mesoporous metal oxides including the main factors affecting their development and the existing challenges.

2. A brief overview of mechanochemical synthesis of metal oxides

Typically, mechanochemical synthesis relies on a direct absorption of mechanical energy released during milling by solid reactants. Impact and friction between balls and reactants provide sufficient energy to initiate and stimulate chemical reactions. A high-energy milling assures intense mechanical stresses and bond breakage leading to structural changes and continuous exposure of reactive layers of atoms at interfaces of reactants, which facilitate chemical reactions. Nowadays, automatic ball mills or grinders are predominantly employed for the synthesis of nanoporous materials instead of the previously used mortar and pestle. Such specially designed electronic devices ensure high-energy reliable milling under well-defined reproducible conditions (Fig. 2).[15]

Mechanochemical concepts seem to be very promising for large scale production and/or modification of porous metal oxides for catalysis, battery technology, adsorption, medicine, and so on.[16–24] In particular, new catalysts have been intensively studied for application in water splitting, organic syntheses, removal of pesticides and dyes from wastewater, and removal of diverse harmful gases and vapors, among others.[25–28] Recently, a facile mechanochemical process, which relied on the dehydration of boehmite in a vibration mill afforded a valuable catalyst – corundum, with a nanoparticle size of $\sim$13 nm and a specific surface area (SSA) of $\sim$140 m^2 g^{-1}.[29] Elsewhere, a mechanochemical reaction between titanium and cupric oxide conducted for 12 h resulted in the formation of nanocrystalline titanium oxide with an average particle size of $\sim$ 20 nm.[30] Mesoporous nanoparticles of tin oxide were obtained *via* a simple manual grinding of stannous chloride, ammonium carbonate and glucose followed by calcination at 600 °C.[31] The as-obtained nanoparticles featured crystallite sizes in the range of 6–12 nm and possessed a

Fig. 2 Schematic illustration of (a) a mortar and pestle, (b) planetary mill, (c) shaker and (d) extruder. Images of the instruments for mechanochemical synthesis: (e) mortar grinder, (f) planetary mills with equipment and (g) mixer mill with equipment.[15]

large surface area of 265 m^2 g^{-1} and an average pore size of 2.1 nm, *i.e.*, pores on the border between micro- and mesopore regions. Elsewhere, a combined mechanochemical and calcination route led to mixed cobalt oxides attractive for the selective catalytic reduction of nitrophenols.[32] Mechanochemistry has also been employed for a *waste free* preparation of perovskites, *e.g.*, $LaMnO_3$ directly from the corresponding metal oxide powders (La_2O_3 and Mn_2O_3).[33] Interestingly, mechanochemical redox-based synthesis using $KMnO_4$, $CoCl_2$ and NaOH without any templates afforded highly porous $Co_xMn_{1-x}O_y$ catalysts with a specific surface area of 479 m^2 g^{-1}, which was higher than the values of the corresponding materials obtained by using other methods including co-precipitation method, sol–gel method or solution redox process (Fig. 3a and b).[16] The BJH (Barrett–Joyner–Halenda) pore size distribution (PSD) calculated for the mechanochemically obtained sample shows the presence of narrow mesopores centered around 3.6 nm (Fig. 3c). Moreover, mechanochemical concepts are increasingly exploited for the synthesis of complex mixed metal oxides[34–36] and metal oxide/carbon composites.[37–39] In particular, they are frequently used for activation of metal oxides.[20,40–44] For instance, mechanochemical activation of fumed complex metal oxides including core–shell nanoparticles caused their aggregation and agglomeration resulting in more compacted structures.[40]

Ball milling has been shown as an efficient technique to synthesize organic or inorganic compounds as well as alter their physicochemical properties.[15,45] In this process, the starting powders are subjected to deformations, fractures, abrasion, cold weld *etc.*, resulting in the reduction of particle size, higher specific surface area, a smaller degree of structure ordering or even amorphization. Crystallinity defined as the level of structure ordering can be used for the evaluation of the structural alterations upon milling. The effects of mechanical milling on the crystallinity, crystallite size, crystalline phases, morphology, and porosity of metal oxides or hydroxides have been frequently examined.[46–48] For instance the high-energy ball milling enabled to tailor crystalline phases of TiO_2 mixtures.[48] Polymorphic transformations were observed from anatase to rutile with TiO_2(II) as the intermediate (Fig. 4). The obtained mixtures possessed even twice higher specific surface area than the starting anatase phase mainly due to the fragmentation of particles. Moreover, the introduced defects upon milling generated oxygen vacancies in the surface and bulk of the resulting oxides. The number of oxygen vacancies increased with milling time and promoted a greater reducibility and oxygen mobility in the TiO_2 supports. Overall, these alternations improved the properties making these materials attractive catalyst supports.

3. Soft templating synthesis of mesoporous oxides

To prepare mesoporous silicon- or metal oxides *via* soft templating methods, hydrogen-bonding formation or sufficient charge interactions between precursors and templates are required. Four different models of charge attractions can be distinguished: S^-I^+, S^+I^-, $S^+X^-I^+$, and $S^-X^+I^-$, where S represents a surfactant, I refers to inorganic species, and X represents a mediator.[49] One of these models was successfully implemented in the synthesis of metal

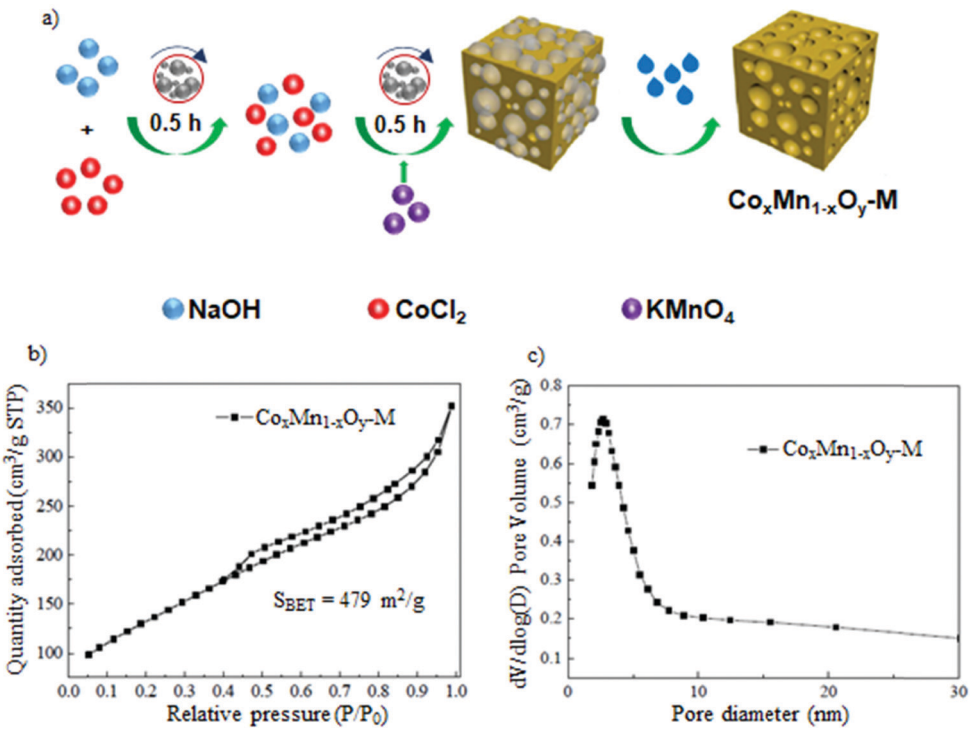

Fig. 3 (a) Schematic illustration of the redox-based strategy for the preparation of mesoporous $Co_xMn_{1-x}O_y$ catalyst, (b) N_2 adsorption–desorption isotherm and (c) PSD function determined for this material. Reproduced with permission from ref. 16 Copyright © 2020 Elsevier B. V.

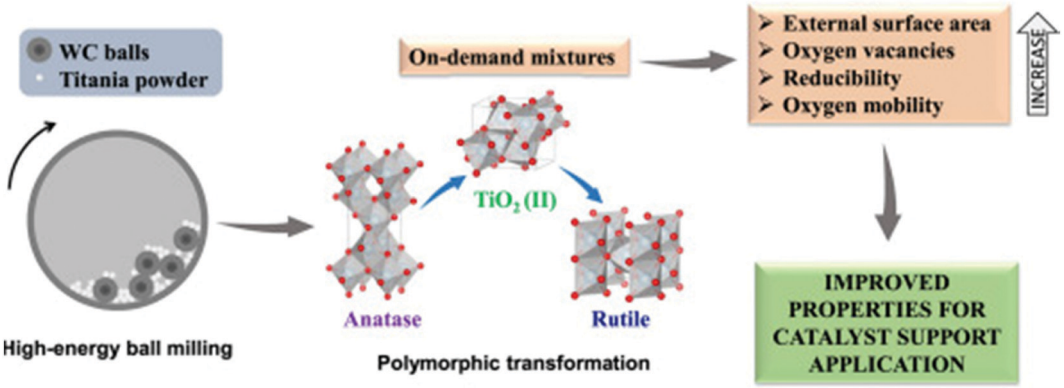

Fig. 4 Schematic illustration of the mechanochemically induced polymorphic transformation of TiO_2 crystalline phases. Reproduced with permission from ref. 48 Copyright © 2020 Elsevier Ltd.

oxide/phosphate mesophases in 1994.[50] However, mesoporous frameworks were not obtained then, because of their collapse upon the thermal removal of the surfactant used. A year later the first synthesis of non-siliceous ordered mesoporous oxide, *i.e.*, titanium oxide with hexagonally arranged mesopores was reported by Antonelli and Ying.[51] They applied calcination at 350 °C, which enabled a successful removal of the template and afforded a metal oxide framework with specific surface area of 200 $m^2\ g^{-1}$. The synthesis involved a modified sol–gel method using titanium alkoxides and phosphate surfactants. Afterwards, these authors synthesized ordered mesoporous niobium oxide characterized by a high surface area of 434 $m^2\ g^{-1}$ and narrow PSD with the maximum at 2.7 nm.[52]

Composite mesophases consisting of surfactant and oxide precursors can be synthesized directly or indirectly *via* electrostatic complementarity between inorganic species dissolved in solution and charged surfactants under specific pH conditions. Diverse surfactants can be used for the synthesis of mesoporous materials. They can form one or more different mesostructures, depending on the synthesis conditions. The geometry of the resulting oxides depends on the morphology of the formed composite mesophases regardless of their compositions. Among various surfactants and block copolymers, the most commonly utilized are alkyltrimethylammonium bromide surfactants, Pluronic-type triblock copolymers *e.g.*, poly(ethylene oxide)-*b*-poly(propylene oxide)-*b*-poly(ethylene oxide), PEO-PPO-PEO and high molecular weight diblock copolymers *e.g.*, polystyrene-*b*-poly(4-vinylpyridine), PS-P4VP or polystyrene-*b*-poly(ethylene oxide), PS-PEO.[53–55] Such diblock, triblock, or even more complex copolymers have the ability to self-assembly into micellar systems similarly as surfactants. Among them, the commercially available Pluronic triblock copolymers F127 and P123 composed of the central block of poly(propylene oxide) PPO and end blocks of poly(ethylene oxide) PEO, $PEO_{106}PPO_{70}PEO_{106}$ and $PEO_{20}PPO_{70}PEO_{20}$, respectively, are the most popular templates for the preparation of mesoporous oxides and other OMMs because of their: (i) ability to form stable micelles in aqueous solutions, (ii) simple removal by heating, and (iii) relatively low price. Schematic illustration of a soft templating strategy using di- and triblock copolymers for the synthesis of inorganic mesoporous materials is presented in Fig. 5. Since the late nineties, block copolymer templating has been shown to be a universal strategy for synthesizing various mesoporous metal oxides with semi-crystalline frameworks including TiO_2, ZrO_2, Nb_2O_5, Ta_2O_5, Al_2O_3, SiO_2, SnO_2, WO_3, and HfO_2, and mixed metal oxides *e.g.*, $SiAlO_y$, Al_2TiO_y, $ZrTiO_y$, $SiTiO_y$, and ZrW_2O_y.[9]

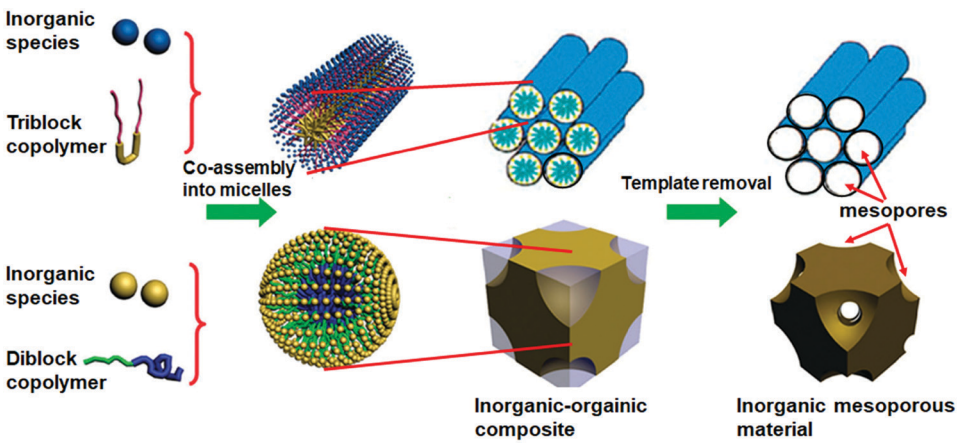

Fig. 5 Schematic representation of a soft templating strategy for the synthesis of inorganic mesoporous materials including metal oxides.[55]

It is still challenging to achieve high crystallinity and preserve the mesoporous structure of metal oxides because it is difficult to control hydrolysis and condensation of their precursors. Thermal treatment, which is applied to remove soft templates and achieve the desired crystallinity, may result in the porous framework collapse.[50,55] Metal oxides are usually susceptible to phase transitions, hydrolysis and/or redox reactions in contrast to more chemically stable silicas, which can be assembled from flexible tetrahedral building blocks. Therefore, one of the most commonly used paths to obtain the soft templated metal oxides is the evaporation induced self-assembly (EISA) of their precursors in the presence of Pluronic-type block copolymers in ethanol to reduce their hydrolysis rate. This strategy was successfully implemented to synthesize ordered mesoporous aluminas[56] and alumina-based mixed metal oxides[57] using aluminum isopropoxide as a precursor. For instance, such mesoporous alumina sample showed good mesoscopic order evidenced by low-angle XRD analysis, which can be attributed to its *p6mm* hexagonal symmetry according to TEM imaging.[56] It possessed a high surface area of 430 $m^2\ g^{-1}$, pore volume of 0.80 $cm^3\ g^{-1}$ and relatively narrow pore-size distribution (4–6 nm). However, its wide-angle XRD patterns revealed the amorphous nature of its pore walls. It is often difficult to transform metal oxide mesostructures into crystalline forms upon heating. The key problem is associated with thermal decomposition of the Pluronic template before achieving the desired crystallinity. To avoid this problem a ligand-assisted synthesis[58] or modified precursor strategy[59] were developed. In these approaches, strong interactions between block copolymers and modified precursors lead to their assembly into ordered mesostructures, the heating of which in a neutral atmosphere generate an *in situ* protective carbon scaffold that preserve mesoporosity of the resulting composite during crystallization. At the end, the carbon scaffold is removed upon heating in air. For instance, the synthesis of mesostructured crystalline titania involved the reaction of titanium isopropoxide and acetylacetone to produce a titanium acetylacetone complex, whose copolymer-assisted assembly followed by carbonization afforded carbon–titania composites.[59] The subsequent removal of the carbonaceous component upon calcination gives rise to the mesoporosity of the resulting crystalline titania.

Another approach to synthesize crystalline mesoporous metal oxides is the assembly of small-sized metal oxide nanocrystals in the presence of block copolymers in non-aqueous media. For instance this approach afforded mesostructured crystalline oxides of tin[60] and cerium.[61] Synthesis of crystalline SnO_2 nanoparticles with a diameter of about 3.5 nm and narrow PSD was reported by Antonietti *et al.*[60] Such small nanoparticles can be further transferred into a stable sol in tetrahydrofurane (THF), and in this form can serve as building blocks in copolymer-assisted synthesis of crystalline mesoporous tin oxide. The as obtained SnO_2 sample featured large mesopores of about 20 nm in a cubic-like arrangement. Elsewhere, a similar strategy afforded crystalline mesoporous CeO_2, the synthesis of which involved the use of a block copolymer and crystalline nanoparticles of this oxide without any additional surface functionalization agents.[61] The nanoparticle sol in an ethanol/water mixture was added to that dispersed in an alcoholic solution hydrogenated polybutadiene–poly(ethylene oxide) (PHB–PEO) block copolymer. Their cooperative assembly into a mesophase was induced by evaporating the solvent. This approach led to a stable (upon calcination at 500 °C) mesostructured crystalline CeO_2 with ordered pores in the size range of 10–12 nm. An analogous strategy was reported for the polymer-assisted synthesis of mesoporous crystalline alumina in aqueous phase by using peptized boehmite nanoparticles.[62,63] The sufficient fragmentation of boehmite particles into nano-sized ones was achieved by conventional heating or microwave irradiation in diluted nitric acid. The resulting boehmite small nanocrystals had the ability to self-assembly with a Pluronic copolymer leading to mesoporous γ-alumina with a large pore volume of $\sim$1.1 $cm^3\ g^{-1}$ and high crystallinity obtained by heating at 400 °C. This procedure can be extended for the synthesis of various alumina-based metal oxides, *e.g.*, $MeAl_2O_4$ (Me = Ni, Co or Cu) (Fig. 6).[63]

Most of the reported synthesis methods of mesoporous metal oxides are complex and based on the usage of solvents, thus require a solvent evaporation step, which prolongs the whole procedure often to several days. Certainly, the mass production of metal oxides and silicas should be developed to meet *green* chemistry requirements. The great promise toward a more environmentally friendly synthesis of functional porous materials gives mechanochemistry, ultrasound-assisted procedures,[64] and the methods rely on fast microwave[63] or UV-irradiation.[65] Mechanochemical synthesis has been shown as a good alternative to multistep solution-based methods for the preparation of organic compounds and advanced nanoporous inorganics including metal oxides.[15,66–69] It is usually performed *via* ball milling under solvent-free conditions or with the addition of small amounts of solvents. Thus, it creates opportunities to conduct reactions with insoluble metal oxide sources, which are difficult to achieve through traditional solvent-based methods.

Sufficient interactions and diffusion between metal oxide precursors and surfactants can be promoted by the kinetic energy and frictional heating released during ball milling. For instance, the recently reported facile ball milling of boehmite with a small amount of diluted nitric acid afforded small boehmite nanocrystals, whose subsequent block copolymer-assisted self-assembly generated mesostructures upon milling (Fig. 7).[70] After direct thermal treatment at 400 °C, a pure crystalline mesoporous alumina (γ phase) with high specific surface area of 390 $m^2\ g^{-1}$ and large pore volume of 1.6 $cm^3\ g^{-1}$ was obtained. To avoid the abrasion of milling balls and vessels, which may contaminate milling products, milling equipment made of silicon nitride was employed.

Designing high-entropy materials, which contain five or even more metal species, is quite a new concept. The introduction of additional metals into metal oxides may require high temperatures. Such structures usually feature limited surface area ($<$30 $m^2\ g^{-1}$).[71,72] Especially challenging is the synthesis of mesoporous high-entropy metal oxides, because their porous frameworks may collapse upon thermal treatment. Ball milling has emerged as an optimal solution because the generated local

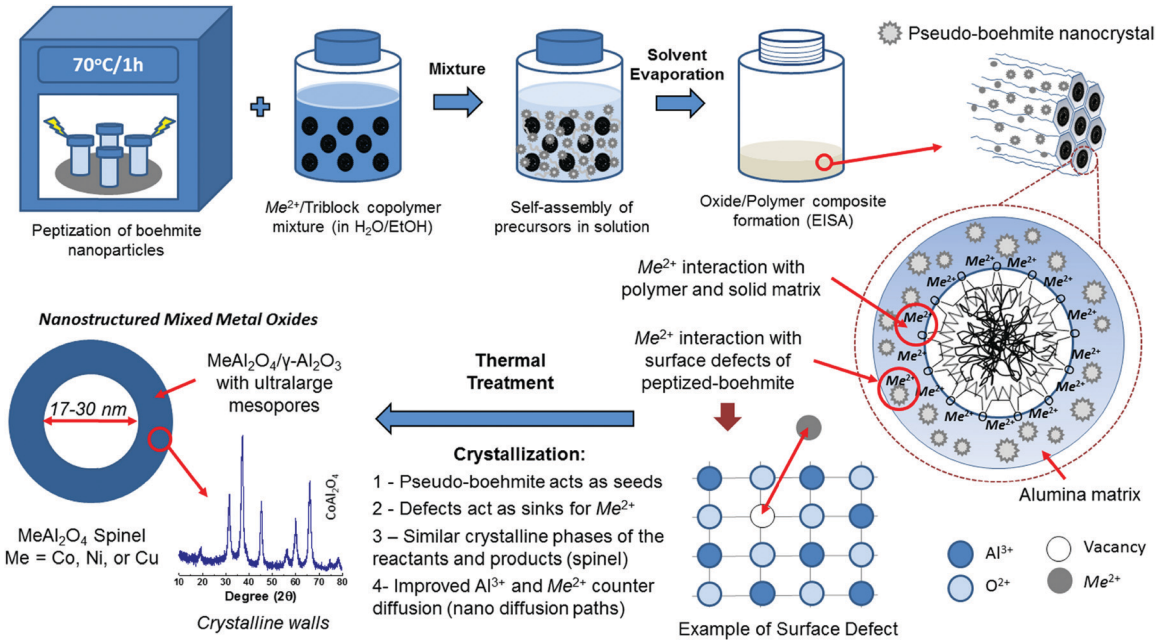

Fig. 6 Schematic illustration of a microwave-assisted synthesis of mesoporous crystalline transition metal aluminates supported on γ-Al_2O_3 ($MeAl_2O_4$/γ-Al_2O_3). Reproduced from ref. 63 published under an ACS Author Choice License. Copyright © 2018 American Chemical Society.

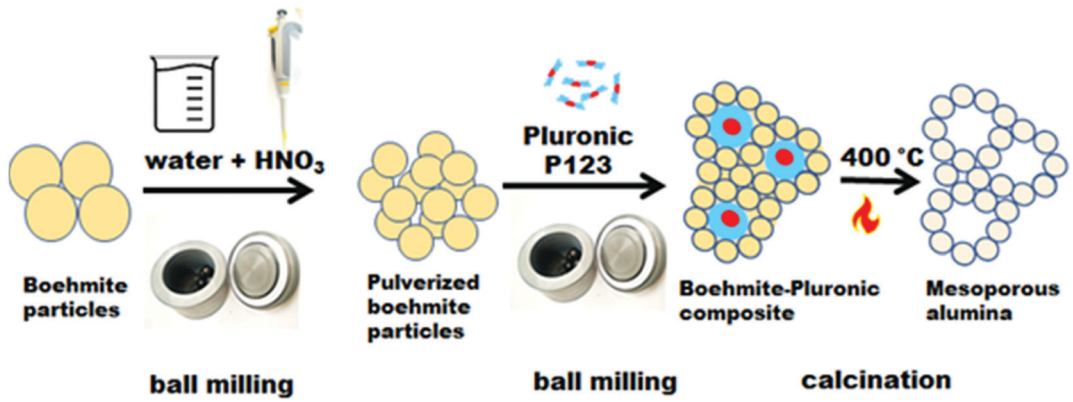

Fig. 7 Schematic illustration for a mechanochemical synthesis of mesoporous alumina. Reproduced with permission from ref. 70. Copyright © 2020 Elsevier Ltd.

short-range heating can be sufficient for the synthesis of high-entropy materials without the deterioration of their porosity. Recently, mesoporous Al_2O_3 (meso-Al_2O_3) with a high SSA of 640 $m^2\ g^{-1}$, a pore volume of 0.75 $cm^3\ g^{-1}$ and a narrow PSD with predominant pore size around 5 nm was successfully obtained by a fast, mechanochemical nonhydrolytic sol–gel method using aluminum isopropoxide as the alumina precursor and Pluronic P123 as the soft template.[73] This synthetic approach afforded various mesoporous aluminum-supported binary oxides, such as CuO_x–Al_2O_3 and MnO_x–Al_2O_3 and even five metal-aluminum oxide (CuNiFeCoMg)O_x–Al_2O_3 (Fig. 8). The preparation of the multimetalic oxides relied on 1 h ball milling at a vibrational frequency of 30 Hz of all the reagents: aluminum isopropoxide, soft template (Polyethylene glycol, PEG-4000) and the corresponding anhydrous metal chlorides. After calcination at 400 °C, high-entropy oxides were obtained, whose porosity was comparable to those obtained by a traditional wet chemistry method. For instance, (CuNiFeCoMg)O_x–Al_2O_3 showed SSA of 200 $m^2\ g^{-1}$ and high catalytic activity for CO oxidation and superior SO_2 tolerance (1000 ppm SO_2 at 280 °C) compared to CuO–Al_2O_3. The results indicate uniform mixing of multimetalic oxides with Al_2O_3 support, thus it is likely that upon the preformed mechanochemical and calcination processes, solid solution was formed. Elsewhere, a similar mechanochemical procedure was employed to synthesize platinum decorated meso-Al_2O_3, where together with the P123 template and $Al(OCHCH_3CH_3)_3$, acetylacetonate platinum ($Pt(acac)_2$) was added in a milling vessel as a noble metal precursor.[74] The as-obtained meso-Al_2O_3 supported Pt (1 wt%) catalyst calcined at 400 °C featured high porosity (SSA of 497 $m^2\ g^{-1}$ and pore volume of 0.55 $cm^3\ g^{-1}$), narrow PSD

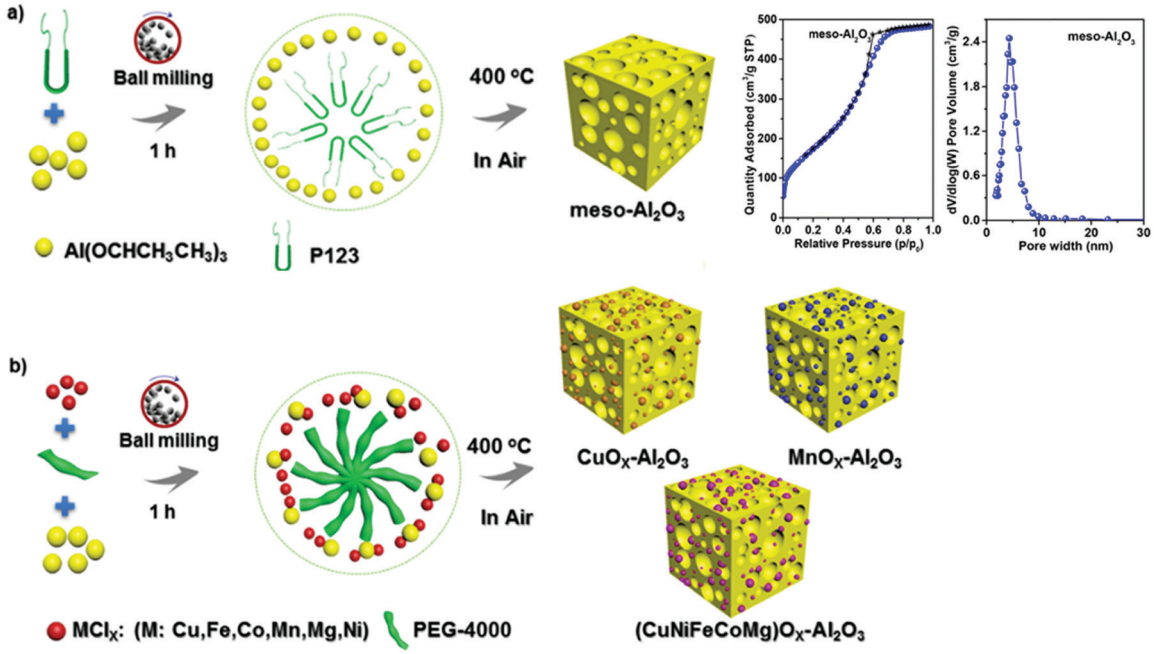

Fig. 8 Schematic illustration of a mechanochemical method for the synthesis of (a) mesoporous Al_2O_3 (meso-Al_2O_3) with the inserted N_2 adsorption–desorption isotherms and PSD function determined for this material, and (b) mesoporous mixed metal oxides. Reproduced with permission from ref. 73. Copyright © 2019, American Chemical Society.

centered around 4 nm and superior activity in the selective hydrogenation of nitrobenzene to aniline.

Mesoporous iron oxides were also successfully prepared through a facile mechanochemical Pluronic-assisted assembly of iron species (Fig. 9).[75] Briefly, the solvent-free high-speed vibrating ball milling of $Fe(NO_3)_3{\cdot}9H_2O$ and Pluronic P123 within 0.5 h followed by calcination at 300 or 400 °C afforded Fe_xO_y with surface areas of up to 149 $m^2\ g^{-1}$ and abundant well-defined mesopores from the range of 2–10 nm. Furthermore, this solid state synthesis was extended for the synthesis of the related Pt-decorated materials with high dispersion of Pt species at the nanometer level (even 1 nm) just by adding H_2PtCl_6 to the reaction vessel. The as-obtained Pt–Fe_xO_y catalysts showed an enhanced activity for oxidation of propylene and CO. Elsewhere, mesoporous Fe_xO_y with a SSA of up to 170 $m^2\ g^{-1}$ was obtained *via* an analogous mechanochemical procedure using cetyltrimethylammonium bromide (CTAB) as the mesopore-directing agent.[76] Calcination at 300 °C for 2 h was sufficient for the thermal removal of the CTAB template, which decomposes at around 250 °C. Adding chloroauric acid ($HAuCl_4$) together with

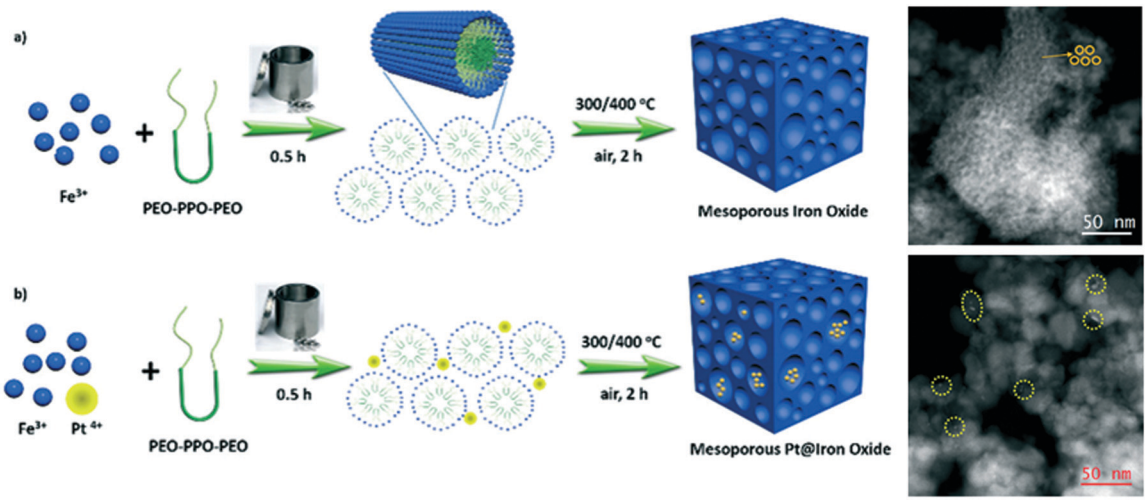

Fig. 9 Schematic illustration of the mechanochemical synthesis of mesoporous iron oxides and Pt-decorated iron oxides *via* solid-state assembly between inorganic species and soft template Pluronic P123 with the inserted STEM-HAADF (scanning transmission electron microscopy in high-angle annular dark field) images.[75]

$Fe(NO_3)_3{\cdot}9H_2O$ and CTAB in the milling vessel led to Au-decorated mesoporous Fe_3O_4 with highly dispersed Au nanoparticles with an average particle size of ~4 nm.

4. Hard (salt) templating synthesis of mesoporous oxides

For over 10 years since the successful synthesis of ordered mesoporous materials, the synthesized ordered mesoporous oxides possessed amorphous or semi-crystalline pore walls, which impeded their applications.[9,56,77–80] Hard templating strategies afforded the first crystalline ordered mesoporous metal oxide α-Fe_2O_3 in 2006.[81] This synthesis involved an impregnation step that relied on the stirring in ethanol of both substrates $Fe(NO_3)_3{\cdot}9H_2O$ and ordered mesoporous silica (KIT-6) used as a hard template. The subsequent heating at 600 °C for 6 h afforded atomic order within the pore walls assuring high crystallinity. After silica removal by using 2 M hot NaOH solution, the as-obtained crystalline α-Fe_2O_3 featured long-range ordering of pores, which originated from relatively strong interactions between iron ions along pore walls. Hard templating strategies are analogous to the casting process of a key with a mold (Fig. 10).[82] Mesostructured silica materials such as MCM-48, SBA-15, SBA-16, and KIT-6 are most often used for synthesizing mesoporous metal oxides *via* wet hard templating due to their highly ordered tunable porosity. Moreover, surface silanol groups (Si–OH) in silicas enhance interactions with metal precursors assuring better replication. The specific features of the resulting products such as pore shape, size and pore ordering are mainly determined by the intrinsic structure of the hard template and applied synthesis conditions. Detailed procedures for the solvent-based syntheses of hard templated ordered mesoporous metal oxides can be found elsewhere.[82,83]

Although a hard templating strategy can be used to obtain a variety of ordered mesoporous metal oxides, its broader applicability is hampered, because it is usually a multistep time-consuming process, which requires specific silica templates that need to be removed under concentrated acidic (HF) or base (NaOH) conditions. Moreover, such harsh conditions of the template removal step can be destructive for vulnerable metal oxide frameworks. Replacement of silicas by mesostructured carbons eliminates problems with using HF or NaOH solutions, because carbonaceous templates can be burnt off, but can result in the reduction of some metal oxides and/or formation of metal carbides.

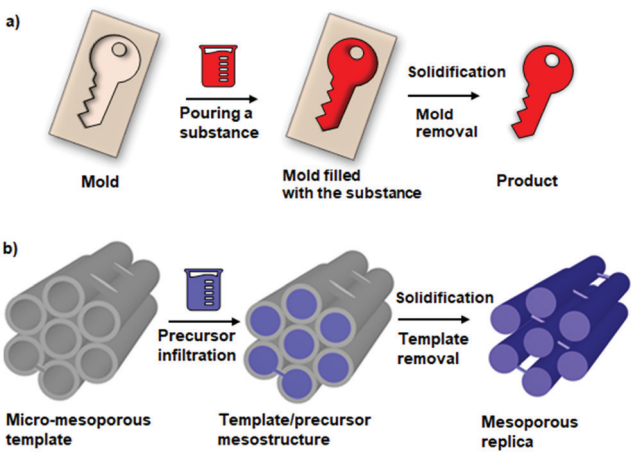

Fig. 10 (a) Schematic illustration of the similarities of the casting process of a key with a mold and (b) hard templating method for synthesizing mesoporous materials. Adapted from ref. 82 published under an ACS Author Choice License. Copyright © 2017 American Chemical Society.

Overall, both templating methods for synthesizing mesoporous metal oxides are predominantly performed in solutions, and thus require solvents, soluble metal oxide precursors, and usually a long time for drying. Recently, a mechanochemical procedure was successfully developed to overcome some weaknesses of the solvent-based hard templating. Briefly, a solvent free 1 h vibrating ball milling of metal oxide precursors and commercial SiO_2 followed by calcination and template removal afforded diverse crystalline mesoporous metal oxides (Fig. 11).[84] Afterwards, the silica template needs to be removed in 2.5 M NaOH for 8 h, repeated four times. This procedure enabled a series of crystalline mesoporous metal oxides with high porosity to be obtained, *e.g.*, ZrO_2 (SSA of 293 $m^2\ g^{-1}$), Fe_2O_3 (SSA of 163 $m^2\ g^{-1}$), CeO_2 (SSA of 211 $m^2\ g^{-1}$) and also mixed metal oxides CuO_x–CeO_y with a SSA of 237 $m^2\ g^{-1}$ and CuO_x–CoO_y–CeO_z with a SSA of 203 $m^2\ g^{-1}$. The as-obtained mixed metal oxides showed great performance as catalysts for CO oxidation (Fig. 11e). Nevertheless, the calculated PSDs by the BJH model for most samples were broad and centered around 12 nm, which roughly reflected the particle size of the silica template. Moreover, according to the recorded XRD patterns, their crystallinity is rather low.

Instead of the colloidal silica template, aluminum hydroxide can also serve as the mesopore-directing agent under milling.[85] Interestingly, milling a mixture of aluminum hydroxide and metal oxide precursors led to the formation of aluminum hydroxide/metal oxide composites with uniform distribution of Al and metal cationic oxides. Subsequent calcination of these composites resulted in alumina/metal oxide mesostructures, which even without removal of alumina could be used as alumina-supported catalysts for many reactions. However, washing these composites in 1 M NaOH solution at 60 °C for 12 h repeated three times was used to remove the alumina template and obtain Al-free metal oxide porous frameworks. This approach was used to obtain a series of crystalline mesoporous metal oxides with relatively high surface area *e.g.*, Fe_2O_3 (SSA of 280 $m^2\ g^{-1}$), Co_3O_4 (SSA of 155 $m^2\ g^{-1}$), CeO_2 (SSA of 192 $m^2\ g^{-1}$), ZrO_2 (SSA of 170 $m^2\ g^{-1}$) and mixed metal oxides *e.g.*, CuO_x–CeO_y (SSA of 177 $m^2\ g^{-1}$), FeO_x–CeO_y (SSA of 170 $m^2\ g^{-1}$), CoO_x–CuO_y–CeO_z (SSA of 154 $m^2\ g^{-1}$) or CoO_x–FeO_y–CeO_z (SSA of 133 $m^2\ g^{-1}$). Although this synthesis method is feasible and effective, the resulting metal oxides possess quite broad pore-size distributions as evidenced by those shown in Fig. 12d.[85] Further studies are needed toward synthesizing metal oxides with uniform porosity, which would require the use of well-defined templates. For instance, in the case of colloidal templating the monodispersed and non-aggregated nanoparticles should be used as templates.

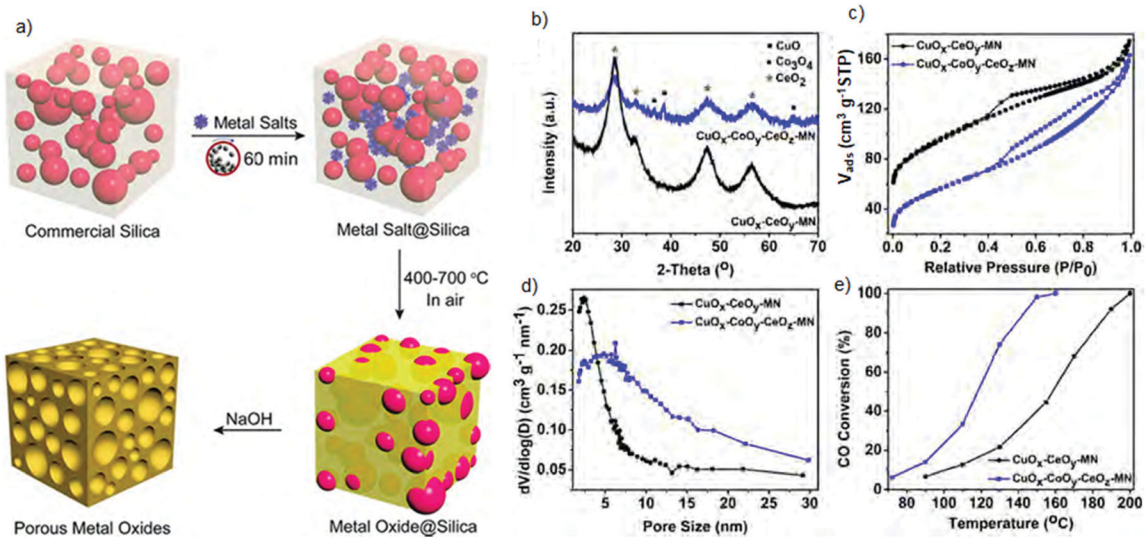

Fig. 11 (a) Schematic illustration of the hard templating synthesis of mesoporous metal oxides using commercial silica as the template, (b) XRD patterns, (c) nitrogen adsorption–desorption isotherms, (d) PSD functions and (e) CO conversion profiles of the as-prepared mixed metal oxides. Reproduced with permission from ref. 84 Copyright © 2018, American Chemical Society.

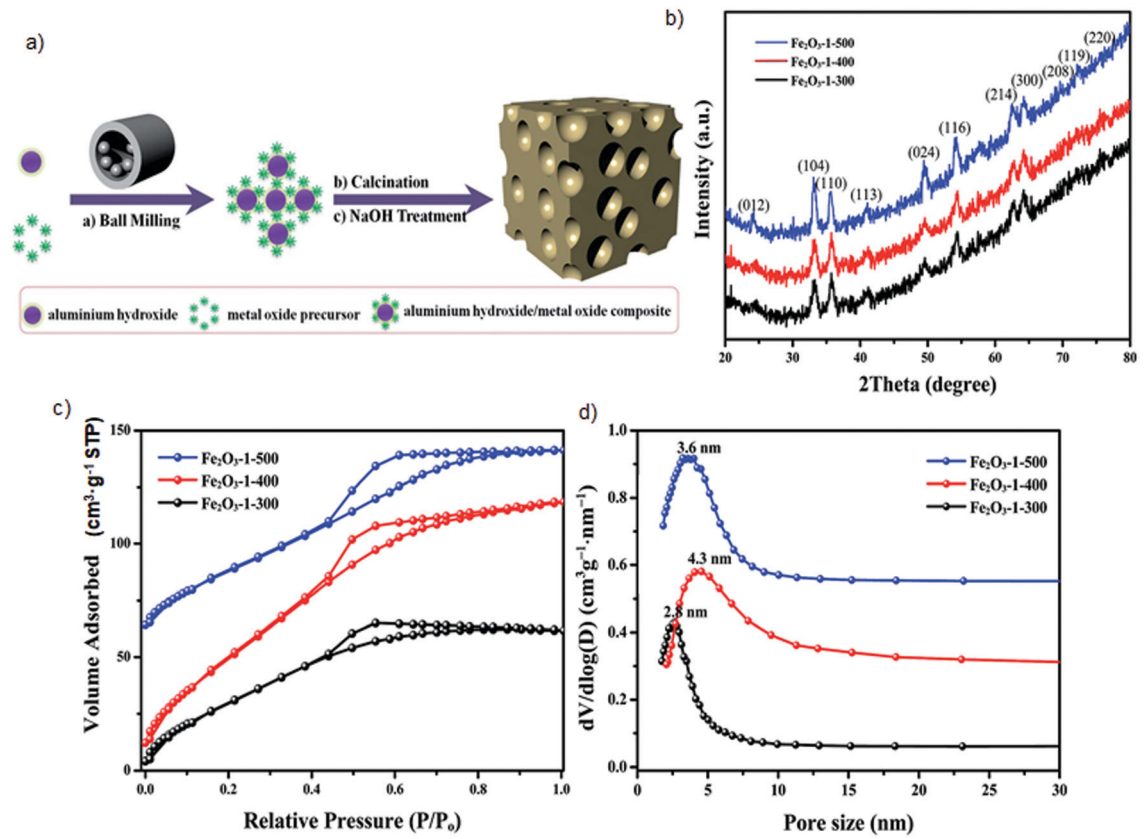

Fig. 12 (a) Schematic illustration of aluminum hydroxide-directed mechanochemical synthesis of mesoporous crystalline metal oxides, (b) XRD patterns, (c) low-temperature N_2 adsorption–desorption isotherms, and (c) PSD determined for Fe_2O_3 prepared at different calcination temperatures.[85]

From environmental and economic viewpoints, the salt templating strategy seems to be a better alternative for the preparation of mesoporous solids than hard templating involving the use of siliceous templates because non-carbonizable salts can be easily removed by post-synthetic washing in water, diluted acids or bases. Moreover, the salt templating can be performed through mechanochemical reactions. Recently, a general route was reported for a facile environmentally-friendly synthesis of

diverse porous metal oxides and the corresponding supported metal oxides with well-dispersed noble metal nanoparticles based on mechanochemically-assisted salt templating.[86] The synthesis procedure afforded transition metal oxides such as Co_3O_4, Fe_xO_y, and Cr_2O_3 by performing an initial solvent-free ball milling of NaCl particles with transition metal precursors for 0.5 h to prepare a solid solution and further 0.5 h milling after the addition of NaOH. The subsequent steps of calcination in air and washing in water led to mesoporous metal oxides with SSA up to 224 m^2 g^{-1} (Fig. 13a). Also, the noble metal Rh-, Pd- or Pt-decorated samples were prepared this way by adding the corresponding noble metal chlorides to the milling vessel containing NaCl and transition metal chlorides. NaCl templates as a non-carbonizable salt can be simply recycled by washing in water at the end of the synthesis, hence additional pores are generated in the frameworks. In this approach, NaCl served as an ion-sharing platform, which enabled to dilute noble metal ions. Thus, the addition of the salt template was essential not only to create an additional mesoporosity but also to disperse noble metal species within the transition metal oxides. This procedure enabled incorporation of small-sized Pd or Pt nanoparticles into mesoporous frameworks of Co_3O_4, Fe_xO_y, and Cr_2O_3 with an average size of 3.1–3.2 nm yielding efficient catalysts *e.g.*, for CH_4 combustion, hydrogenation of nitrobenzene and derivatives, and reversed water gas shift reaction (Fig. 13b). Although, salt templating seems to be a facile and quite universal strategy, the as-synthesized mesoporous metal oxide frameworks feature broad pore distributions, as shown in Fig. 13c,d for Co_2O_3 as an example.

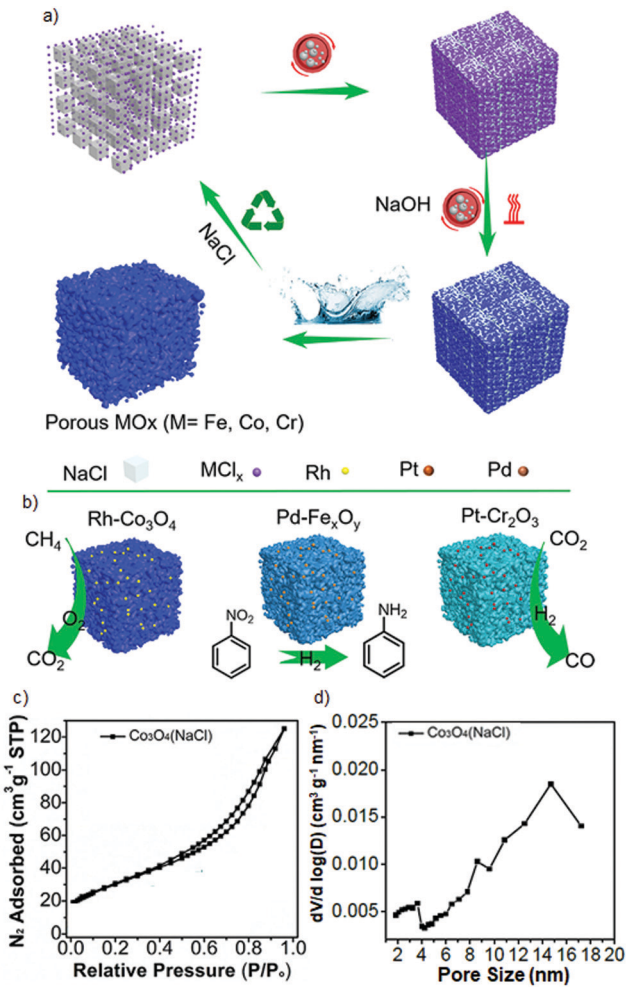

Fig. 13 (a) Schematic illustration of the versatile synthesis of porous metal oxides and the corresponding supported metal oxides *via* a salt templating method, (b) schematic structures of as-prepared noble-metal containing catalysts and examples of their application in model redox reactions, (c) low-temperature N_2 adsorption–desorption isotherm and (d) PSD determined for Co_2O_3. Reproduced with permission from ref. 86 Copyright © 2020 Elsevier Inc.

Elsewhere, polyoxometalates (POMs) have been shown to be efficient bifunctional templates for the synthesis of mesoporous oxides with reactive surfaces.[87] A facile mechanochemical strategy using POMs and the corresponding metal salts afforded mesoporous metal oxides such as Co_3O_4, Fe_3O_4, NiO, La_2O_3, MnO_2, CeO_2, ZrO_2, and CuO with surface areas up to 210 m^2 g^{-1} (Fig. 14a). Ion-sharing between metal precursors and large POM clusters upon milling led to $M_x(POM)_y$-containing ionic composites, whose pyrolysis and subsequent removal of POM by washing with water gave mesoporous oxides. Nevertheless, the complete removal of POM requires an additional washing with 0.5 M NaOH solution. Such obtained mesostructures showed higher activity in CO oxidation than hard templated or commercial metal oxides, thanks to the oxidative feature of POMs, which contributed to the formation of high valence metal cations on their surfaces. This strategy seems to be convenient for the synthesis of various useful mesoporous metal oxides. However, the as-obtained materials feature rather low crystallinity and broad PSDs (Fig. 14b and c). For instance, the XRD pattern of mesoporous Co_3O_4 synthesized by using POM as a template, denoted as Co_3O_4(PMo), shows low intensity peaks related to the planes of its cubic phase, which are even lower than those recorded for Co_3O_4 prepared in a similar way but using commercial silica as a template – denoted as Co_3O_4(Si) (Fig. 14b). These differences were assigned to the larger crystallite size of Co_3O_4(Si), compared with Co_3O_4(PMo), for which the average particle size calculated by Scherrer's equation were estimated to be about 16 nm and 6 nm, respectively. On the other hand, the PSD curve determined for Co_3O_4(PMo) also suggests the formation of larger pores, *i.e.*, those in the range of macropores (Fig. 14c). Apparently, the use of diverse large/complex clusters as templates in the mechanochemical synthesis may afford macroporous metal oxides.

Table 1 summarizes the reviewed mesoporous metal oxides obtained *via* mechanochemistry, their synthesis and proposed applications.

Mechanochemistry has also been utilized for the incorporation of catalytically active metals or metal oxides such as Al,[88] Nb,[89,90] Pd,[91] $(Fe\text{-}Co)_3O_4$,[92] Fe_xO_y,[65,93] and Co_3O_4[94] into the frameworks of mesoporous silicas. For instance, low loadings (0.2–0.4 wt%) of Al species can be incorporated into SBA-15 or MCM-41 silicas *via* a simple wet ball milling of the silica with aluminum isopropoxide or a dry milling with small amounts of Al-containing MOFs used as aluminum sources. The as-obtained calcined Al-containing

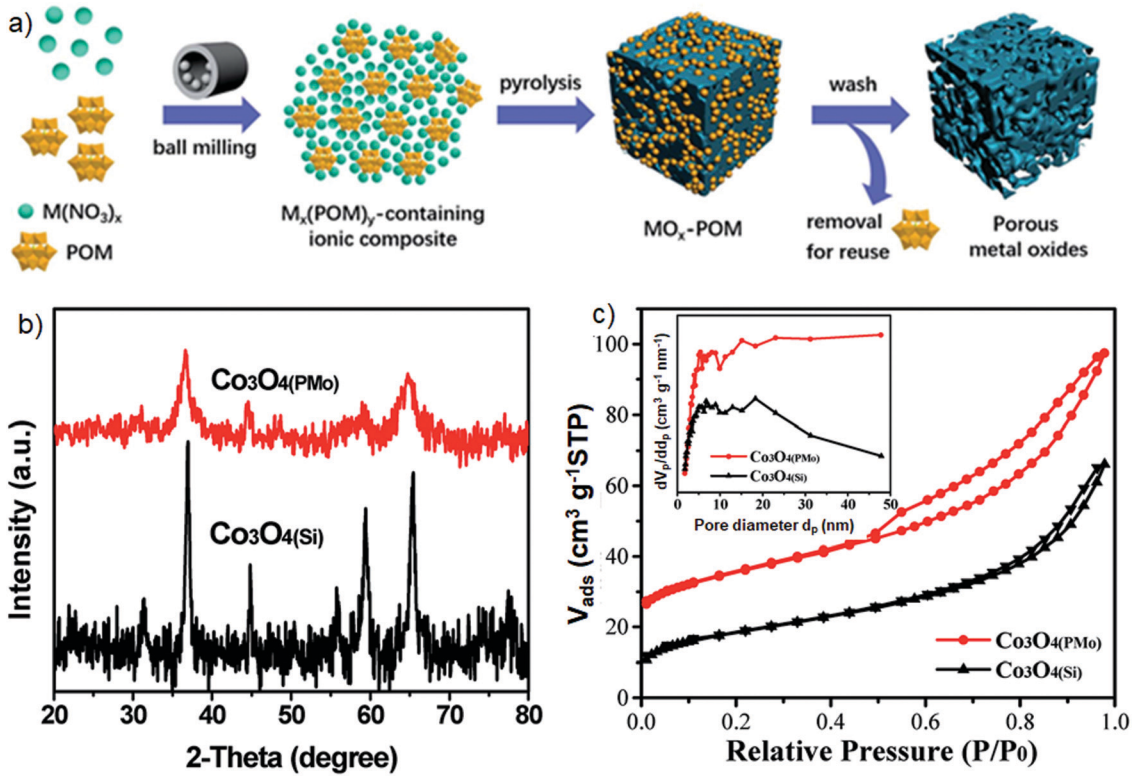

Fig. 14 (a) Schematic illustration of polyoxometalates (POMs) templating mechanochemical synthesis of mesoporous metal oxides, (b) XRD patterns and (c) N_2 adsorption–desorption isotherms with the inserted PSDs obtained for Co_3O_4(PMo) and Co_3O_4(Si). For clarity, the isotherm of Co_3O_4(PMo) is offset along the y-axis by 20 $cm^3STP\ g^{-1}$.[87]

Table 1 Examples of mesoporous metal oxides obtained *via* mechanochemistry, their synthesis and proposed applications

Mechanochemically synthesized mesoporous metal oxides	Templating strategy	Template used	Application	Ref.
Al_2O_3	Soft templating	Pluronic P123	—	70
Al_2O_3, CuO–Al_2O_3, Mn_3O_4–Al_2O_3, Co_3O_4–Al_2O_3, MgO–Al_2O_3, NiO–Al_2O_3, Fe_2O_3–Al_2O_3, (CuNiFeCo)O_x–Al_2O_3 (CuNiFeCoMg)O_x–Al_2O_3	Soft templating	Pluronic P123 or Polyethylene glycol (PEG-4000)	Catalytic CO oxidation	73
Pt-decorated Al_2O_3	Soft templating	Pluronic P123	Catalytic hydrogenation of nitrobenzene to aniline	74
Fe_xO_y and Pt-decorated Fe_xO_y	Soft templating	Pluronic P123	Catalytic oxidation of propylene and CO	75
Fe_xO_y and Au-decorated Fe_xO_y	Soft templating	Cetyltrimethylammonium bromide (CTAB)	Catalytic CO oxidation	76
ZrO_2, Fe_2O_3, CeO_2, CuO_x–CeO_y, CuO_x–CoO_y–CeO_z	Hard templating	Commercial silica	Catalytic CO oxidation	84
Fe_2O_3, Co_3O_4, CeO_2, ZrO_2, CuO_x–CeO_y, FeO_x–CeO_y, CoO_x–CuO_y–CeO_z, CoO_x–FeO_y–CeO_z	Hard templating	Aluminum hydroxide	—	85
Co_3O_4, Fe_xO_y, Cr_2O_3 and their Rh-, Pd- or Pt-decorated counterparts	Salt templating	NaCl	Catalytic CH_4 combustion, hydrogenation of nitrobenzene and derivatives, reversed water gas shift reaction	86
Co_3O_4, Fe_3O_4, NiO, La_2O_3, MnO_2, CeO_2, ZrO_2, CuO	Salt templating	Polyoxometalates (POMs)	Catalytic CO oxidation	87

mesoporous silicas showed enhanced catalytic activities under mild conditions (microwave irradiation and mechanochemical processing) in the oxidation of diphenyl sulfide, isoeugenol or benzyl alcohol.[88] Furthermore, post-synthetic incorporation of *e.g.*, Nb-species into Al-SBA-15 materials can be performed just by milling the Al-SBA-15 support together with niobium ammonium oxalate hydrate at 350 rpm for 10 min.[89,90] After calcination at 400 °C for 4 h, Nb/Al-SBA-15 catalysts with diverse niobium loadings (0.25–1 wt%) were obtained. A similar dry milling approach afforded a mesoporous Al-SBA-15 support with deposited iron oxide nanoparticles.[93,95]

5. Pros and cons of mechanochemical methods

Mechanosynthesis is a green process that facilitates chemical reactions between solids under solvent-free conditions or with

Table 2 Comparison of typical solvent-based and mechanochemical methods. Adapted with permission from ref. 96 Copyright © 2021 Elsevier Ltd

Solvent-based method	Mechanochemical method
✘ High temperature	✔ Room temperature or slightly elevated
✘ Multiple steps (time-consuming)	✔ One pot synthesis (time-saving)
✘ Large amounts of solvents	✔ Solvent-free or small amounts of solvents
✘ Expensive	✔ Cheap and easy (cost-effective)
✘ Large amounts of liquid wastes	✔ Minimum wastes
✔ Highly crystalline products	✘ May lead to amorphization
✔ Basic equipment	✘ Special grinders/mills or mortar and pestle
✔ Pure products	✘ Possible impurities from milling reactors
✔ Precise control of synthesis	✘ Precise control of synthesis is difficult

a small addition of solvents, usually in a short time. Therefore, it reduces solvent consumption and liquid waste accumulation. The mechanical energy delivered to the system is sufficient to initiate chemical reactions without external heating, thus the synthesis can significantly decrease energy requirements. Moreover, this process assures a high reaction yield and gives an opportunity to use insoluble substrates, which is sometimes difficult in solvent-based methods. On the other hand, using mechanochemical methods it is difficult to precisely control the synthesis mechanism. Moreover, fast nucleation and limited control over crystal growth may result in the reduced crystallinity and quality of the obtained products. Table 2 presents a comparison of typical solvent-based and mechanochemical methods.[96]

Although some of the mechanochemically obtained metal oxides discussed here show roughly uniform mesoporosity (often nonuniform), so far it is very difficult to achieve both high crystallinity and ordered arrangement of uniform pores in such structures. So far, this method has been mainly used to obtain the mesostructured metal oxides with disordered pores. For instance, the mechanochemical synthesis of hard templated metal oxides by using ordered mesoporous silicas as templates is challenging.

6. Conclusions

Mesoporous oxides with large uniform pores, high accessible surface area, high thermal stability and crystalline pore walls are of great interest for catalysis and adsorption related applications. It is challenging to obtain mesoporous oxides with controlled pore size distribution, large and accessible surface area, ordered interconnected pores, high conductivity and structural stability *via* facile low-cost and environmentally friendly methods from sustainable precursors. Mechanochemistry has been shown to be a powerful fast and *green* method for preparation of mesoporous metal oxides obtained by using either soft-, hard- or salt templating strategies. Mechanochemically-assisted syntheses of mesoporous oxides, which involve the use of Pluronic block copolymers, CTAB or salts as templates are especially promising for real applications. A large variety of mechanochemically synthesized mesoporous metal oxides, mixed metal oxides, and noble metal decorated metal oxides have been already reported. Among them, mesoporous Al_2O_3, Fe_3O_4, Co_3O_4 and CeO_2 drew attention because of their great potential, especially in the context of heterogenous catalysis. Although some of the mechanochemically obtained metal oxides showed roughly uniform mesoporosity, so far it is difficult to achieve ordered arrangement of the pores in such structures. It seems, that the mechanochemical synthesis of sustainable metal oxides with high crystallinity and tunable ordered porosity remains a challenging task. Intensive studies are recommended to scale-up synthesis *via* environmentally friendly methods to obtain crystalline mesostructured metal oxides with narrow pore size distributions.

Mechanochemistry has been also utilized to alter physicochemical properties of metal oxides or incorporate diverse metallic species into the frameworks of ordered mesoporous silicas. We believe that mechanochemically obtained mesoporous materials and their employment into practical technologies will emerge soon.

Conflicts of interest

There are no conflicts to declare.

Notes and references

1 T. Yanagisawa, T. Shimizu, K. Kuroda and C. Kato, *Bull. Chem. Soc. Jpn.*, 1990, **63**, 988–992.
2 C. T. Kresge, M. E. Leonowicz, W. J. Roth, J. C. Vartuli and J. S. Beck, *Nature*, 1992, **359**, 710–712.
3 J. S. Beck, J. C. Vartuli, W. J. Roth, M. E. Leonowicz, C. T. Kresge, K. D. Schmitt, C. T. W. Chu, D. H. Olson, E. W. Sheppard, S. B. McCullen, J. B. Higgins and J. L. Schlenker, *J. Am. Chem. Soc.*, 1992, **114**, 10834–10843.
4 B. Szcześniak, J. Choma and M. Jaroniec, *Chem. Commun.*, 2020, **56**, 7836–7848.
5 J. Liu, L. Xie, Z. Wang, S. Mao, Y. Gong and Y. Wang, *Chem. Commun.*, 2020, **56**, 229–232.
6 Y. Huang, W. Ho, S. Lee, L. Zhang, G. Li and J. C. Yu, *Langmuir*, 2008, **24**, 3510–3516.
7 J. Wei, Z. Sun, W. Luo, Y. Li, A. A. Elzatahry, A. M. Al-Enizi, Y. Deng and D. Zhao, *J. Am. Chem. Soc.*, 2017, **139**, 1706–1713.
8 W. Li, J. Liu and D. Zhao, *Nat. Rev. Mater.*, 2016, **1**, 16023.
9 P. Yang, D. Zhao, D. I. Margolese, B. F. Chmelka and G. D. Stucky, *Chem. Mater.*, 1999, **11**, 2813–2826.
10 H. Tüysüz, E. L. Salabaş, E. Bill, H. Bongard, B. Spliethoff, C. W. Lehmann and F. Schüth, *Chem. Mater.*, 2012, **24**, 2493–2500.
11 T. Brezesinski, J. Wang, J. Polleux, B. Dunn and S. H. Tolbert, *J. Am. Chem. Soc.*, 2009, **131**, 1802–1809.
12 Z. Zhang, Y. Han, F.-S. Xiao, S. Qiu, L. Zhu, R. Wang, Y. Yu, Z. Zhang, B. Zou, Y. Wang, H. Sun, D. Zhao and Y. Wei, *J. Am. Chem. Soc.*, 2001, **123**, 5014–5021.
13 T. Yu, H. Zhang, X. Yan, Z. Chen, X. Zou, P. Oleynikov and D. Zhao, *J. Phys. Chem. B*, 2006, **110**, 21467–21472.

14 B. Szczęśniak, J. Phuriragpitikhon, J. Choma and M. Jaroniec, *J. Mater. Chem. A*, 2020, **8**, 18464–18491.
15 B. Szczesniak, S. Borysiuk, J. Choma and M. Jaroniec, *Mater. Horiz.*, 2020, **7**, 1457–1473.
16 J. Bao, H. Chen, S. Yang and P. Zhang, *Chin. J. Catal.*, 2020, **41**, 1846–1854.
17 P. Zhang and S. Dai, *J. Mater. Chem. A*, 2017, **5**, 16118–16127.
18 S. Khalameida, K. Wieczorek-Ciurowa and V. Zazhigalov, *Acta Phys. Pol., A*, 2014, **126**, 963–966.
19 T. Friščić, C. Mottillo and H. M. Titi, *Angew. Chem., Int. Ed.*, 2020, **59**, 1018–1029.
20 B. Fotoohi and S. Blackburn, *J. Eur. Ceram. Soc.*, 2012, **32**, 2267–2272.
21 K. Kucio, B. Charmas, S. Pasieczna-Patkowska and M. Zięzio, *Appl. Nanosci.*, 2020, **10**, 4733–4746.
22 B. Medina, M. G. Verdério Fressati, J. M. Gonçalves, F. M. Bezerra, F. A. Pereira Scacchetti, M. P. Moisés, A. Bail and R. B. Samulewski, *Mater. Chem. Phys.*, 2019, **226**, 318–322.
23 R. Ambade, R. Chakravarty, J. Bahadur, B. Ganjave, D. Sen, S. Chakraborty and A. Dash, *J. Chromatogr. A*, 2020, **1612**, 460614.
24 B. Rahmanivahid, M. Pinilla-de Dios, M. Haghighi and R. Luque, *Molecules*, 2019, **24**, 2597.
25 C. Xu, S. De, A. M. Balu, M. Ojeda and R. Luque, *Chem. Commun.*, 2015, **51**, 6698–6713.
26 M. Zhong, J. Zhai, Y. Xu, L. Jin, Y. Ye, H. Hu, F. Ma and X. Fan, *Fuel*, 2020, **263**, 116763.
27 A. K. Vasudevan, M. Schoenitz and E. L. Dreizin, *Appl. Catal., A*, 2020, **601**, 117604.
28 A. Ochirkhuyag, A. Sápi, Á. Szamosvölgyi, G. Kozma, Á. Kukovecz and Z. Kónya, *Phys. Chem. Chem. Phys.*, 2020, **22**, 13999–14012.
29 A. P. Amrute, Z. Łodziana, H. Schreyer, C. Weidenthaler and F. Schüth, *Science*, 2019, **366**, 485–489.
30 T. Anuradha and S. Ranganathan, *Bull. Mater. Sci.*, 2007, **30**, 263–269.
31 R. Chakravarty, S. Chakraborty, R. Shukla, J. Bahadur, R. Ram, S. Mazumder, H. Dev Sarma, A. K. Tyagi and A. Dash, *Dalton Trans.*, 2016, **45**, 13361–13372.
32 L. Shultz, B. McCullough, W. Newsome, H. Ali, T. Shaw, K. Davis, F. Uribe-Romo, M. Baudelet and T. Jurca, *Molecules*, 2019, **25**, 89.
33 R. H. Blackmore, M. E. Rivas, T. Eralp Erden, T. Dung Tran, H. R. Marchbank, D. Ozkaya, M. de Gutierrez, A. Wagland, P. Collier and P. P. Wells, *Dalton Trans.*, 2020, **49**, 232–240.
34 V. V. Zyryanov, *Inorg. Mater.*, 2003, **39**, 1163–1171.
35 V. V. Zyryanov and N. F. Uvarov, *Inorg. Mater.*, 2005, **41**, 281–287.
36 V. V. Zyryanov, V. I. Smirnov and M. I. Ivanovskaya, *Inorg. Mater.*, 2005, **41**, 618–626.
37 L. Xia, Y. Lu, H. Meng and C. Li, *J. Hazard. Mater.*, 2020, **393**, 122487.
38 W. Shan, P. Zhang, S. Yang, H. Zhu, P. Wu, H. Xing and S. Dai, *J. Mater. Chem. A*, 2017, **5**, 23446–23452.
39 S. M. McCullough, C. J. Flynn, C. C. Mercado, A. J. Nozik and J. F. Cahoon, *J. Mater. Chem. A*, 2015, **3**, 21990–21994.
40 V. M. Gun'ko, V. V. Turov, V. I. Zarko, O. V. Goncharuk, E. M. Pakhlov, J. Skubiszewska-Zięba and J. P. Blitz, *Adv. Colloid Interface Sci.*, 2016, **235**, 108–189.
41 M. Wang, Q. Tan and J. Li, *Environ. Sci. Technol.*, 2018, **52**, 13136–13143.
42 A. A. Il'in, R. N. Rumyantsev, K. K. Dao, A. A. Chuyasova, U. S. Uzhevskaya, D. S. Popov and A. P. Il'in, *Glass Ceram.*, 2019, **76**, 145–151.
43 T. Grigoreva, A. Novakova, T. Kiseleva, A. Barinova, A. Ancharov, T. Talako, I. Vorsina, K. Becker, V. Sepelak, S. Tsybulya, O. Bulavchenko and N. Lyakhov, *J. Phys.: Conf. Ser.*, 2009, **144**, 12076.
44 G. Karagedov and N. Lyakhov, *KONA Powder Part. J.*, 2003, **21**, 76–87.
45 B. Szczęśniak, J. Phuriragpitikhon, J. Choma and M. Jaroniec, *J. Colloid Interface Sci.*, 2020, **577**, 163–172.
46 D. A. Giannakoudakis, G. Chatel and J. C. Colmenares, *Top. Curr. Chem.*, 2019, **378**, 2.
47 Y. Wang, S. Luo, Z. Wang and Y. Fu, *Appl. Clay Sci.*, 2013, **80–81**, 334–339.
48 M. G. Rinaudo, A. M. Beltrán, M. A. Fernández, L. E. Cadús and M. R. Morales, *Mater. Today Chem.*, 2020, **17**, 100340.
49 Q. Huo, D. I. Margolese, U. Ciesla, P. Feng, T. E. Gier, P. Sieger, R. Leon, P. M. Petroff, F. Schüth and G. D. Stucky, *Nature*, 1994, **368**, 317–321.
50 Q. Huo, D. I. Margolese, U. Ciesla, D. G. Demuth, P. Feng, T. E. Gier, P. Sieger, A. Firouzi and B. F. Chmelka, *Chem. Mater.*, 1994, **6**, 1176–1191.
51 D. M. Antonelli and J. Y. Ying, *Angew. Chem., Int. Ed. Engl.*, 1995, **34**, 2014–2017.
52 D. M. Antonelli and J. Y. Ying, *Angew. Chem., Int. Ed. Engl.*, 1996, **35**, 426–430.
53 C. Liang, K. Hong, G. A. Guiochon, J. W. Mays and S. Dai, *Angew. Chem., Int. Ed.*, 2004, **43**, 5785–5789.
54 Y. Deng, J. Liu, C. Liu, D. Gu, Z. Sun, J. Wei, J. Zhang, L. Zhang, B. Tu and D. Zhao, *Chem. Mater.*, 2008, **20**, 7281–7286.
55 D. Gu and F. Schüth, *Chem. Soc. Rev.*, 2014, **43**, 313–344.
56 Q. Yuan, A.-X. Yin, C. Luo, L.-D. Sun, Y.-W. Zhang, W.-T. Duan, H.-C. Liu and C.-H. Yan, *J. Am. Chem. Soc.*, 2008, **130**, 3465–3472.
57 S. M. Morris, P. F. Fulvio and M. Jaroniec, *J. Am. Chem. Soc.*, 2008, **130**, 15210–15216.
58 D. Feng, W. Luo, J. Zhang, M. Xu, R. Zhang, H. Wu, Y. Lv, A. M. Asiri, S. B. Khan, M. M. Rahman, G. Zheng and D. Zhao, *J. Mater. Chem. A*, 2013, **1**, 1591–1599.
59 M. Marszewski, J. Marszewska, S. Pylypenko and M. Jaroniec, *Chem. Mater.*, 2016, **28**, 7878–7888.
60 J. Ba, J. Polleux, M. Antonietti and M. Niederberger, *Adv. Mater.*, 2005, **17**, 2509–2512.
61 A. S. Deshpande, N. Pinna, B. Smarsly, M. Antonietti and M. Niederberger, *Small*, 2005, **1**, 313–316.
62 P. F. Fulvio, R. I. Brosey and M. Jaroniec, *ACS Appl. Mater. Interfaces*, 2010, **2**, 588–593.
63 A. A. S. Gonçalves, M. J. F. Costa, L. Zhang, F. Ciesielczyk and M. Jaroniec, *Chem. Mater.*, 2018, **30**, 436–446.
64 J. Deng, L. Zhang, H. Dai, Y. Xia, H. Jiang, H. Zhang and H. He, *J. Phys. Chem. C*, 2010, **114**, 2694–2700.
65 G. Feng, J. Wang, M. Boronat, Y. Li, J.-H. Su, J. Huang, Y. Ma and J. Yu, *J. Am. Chem. Soc.*, 2018, **140**, 4770–4773.

66 M. Leonardi, M. Villacampa and J. C. Menéndez, *Chem. Sci.*, 2018, **9**, 2042–2064.
67 S. R. Chauruka, A. Hassanpour, R. Brydson, K. J. Roberts, M. Ghadiri and H. Stitt, *Chem. Eng. Sci.*, 2015, **134**, 774–783.
68 L. Li, S. Pu, Y. Liu, L. Zhao, J. Ma and J. Li, *Adv. Powder Technol.*, 2018, **29**, 2194–2203.
69 V. Šepelák, S. Bégin-Colin and G. Le Caër, Dalton Trans., 2012, **41**, 11927–11948.
70 B. Szczęśniak, J. Choma and M. Jaroniec, *Microporous Mesoporous Mater.*, 2021, **312**, 110792.
71 A. Sarkar, R. Djenadic, N. J. Usharani, K. P. Sanghvi, V. S. K. Chakravadhanula, A. S. Gandhi, H. Hahn and S. S. Bhattacharya, *J. Eur. Ceram. Soc.*, 2017, **37**, 747–754.
72 H. Chen, J. Fu, P. Zhang, H. Peng, C. W. Abney, K. Jie, X. Liu, M. Chi and S. Dai, *J. Mater. Chem. A*, 2018, **6**, 11129–11133.
73 Z. Zhang, S. Yang, X. Hu, H. Xu, H. Peng, M. Liu, B. P. Thapaliya, K. Jie, J. Zhao, J. Liu, H. Chen, Y. Leng, X. Lu, J. Fu, P. Zhang and S. Dai, *Chem. Mater.*, 2019, **31**, 5529–5536.
74 S. Nie, S. Yang and P. Zhang, *Chem. Eng. Sci.*, 2020, **220**, 115619.
75 M. Zhou, J. Zhao, P. Zhang, N. Chen and S. Yang, *Catal. Sci. Technol.*, 2019, **9**, 3907–3913.
76 J. Zhao, Y. Shu and P. Zhang, *Chin. J. Catal.*, 2019, **40**, 1078–1084.
77 P. Yang, D. Zhao, D. I. Margolese, B. F. Chmelka and G. D. Stucky, *Nature*, 1998, **396**, 152–155.
78 F. Vaudry, S. Khodabandeh and M. E. Davis, *Chem. Mater.*, 1996, **8**, 1451–1464.
79 F. Schüth, *Chem. Mater.*, 2001, **13**, 3184–3195.
80 P. Yang, T. Deng, D. Zhao, P. Feng, D. Pine, B. F. Chmelka, G. M. Whitesides and G. D. Stucky, *Science*, 1998, **282**, 2244–2246.
81 F. Jiao, A. Harrison, J.-C. Jumas, A. V. Chadwick, W. Kockelmann and P. G. Bruce, *J. Am. Chem. Soc.*, 2006, **128**, 5468–5474.
82 X. Deng, K. Chen and H. Tüysüz, *Chem. Mater.*, 2017, **29**, 40–52.
83 Z. Zhang, F. Zuo and P. Feng, *J. Mater. Chem.*, 2010, **20**, 2206–2212.
84 W. Xiao, S. Yang, P. Zhang, P. Li, P. Wu, M. Li, N. Chen, K. Jie, C. Huang, N. Zhang and S. Dai, *Chem. Mater.*, 2018, **30**, 2924–2929.
85 J. Liu, H. Cheng, J. Bao, P. Zhang, M. Liu, Y. Leng, Z. Zhang, R. Tao, J. Liu, Z. Zhao and S. Dai, *J. Mater. Chem. A*, 2019, **7**, 22977–22985.
86 Y. Shu, H. Chen, N. Chen, X. Duan, P. Zhang, S. Yang, Z. Bao, Z. Wu and S. Dai, *Chem*, 2020, **6**, 1723–1741.
87 Y. Leng, J. Liu, Z. Zhang, H. Chen, P. Zhang and S. Dai, *J. Mater. Chem. A*, 2019, **7**, 27297–27303.
88 M. D. Marquez-Medina, S. Mhadmhan, A. M. Balu, A. A. Romero and R. Luque, *ACS Sustainable Chem. Eng.*, 2019, **7**, 9537–9543.
89 M. Blanco-Sánchez, E. Pfab, N. Lázaro, A. M. Balu, R. Luque and A. Pineda, *Front. Chem.*, 2020, **8**, 42.
90 A. Pineda, N. Lázaro, A. M. Balu, A. Garcia, A. A. Romero and R. Luque, *Mol. Catal.*, 2020, **493**, 111092.
91 X. Cheng, D. Wang, J. Liu, X. Kang, H. Yan, A. Wu, Y. Gu, C. Tian and H. Fu, *Nanoscale*, 2018, **10**, 22348–22356.
92 Z. Surowiec, M. Wiertel, M. Budzyński and W. Gac, *Nukleonika*, 2013, **58**, 87–92.
93 A. Pineda, A. M. Balu, J. M. Campelo, A. A. Romero, D. Carmona, F. Balas, J. Santamaria and R. Luque, *ChemSusChem*, 2011, **4**, 1561–1565.
94 A. Pineda, M. Ojeda, A. A. Romero, A. M. Balu and R. Luque, *Microporous Mesoporous Mater.*, 2018, **272**, 129–136.
95 F. Saberi, D. Rodríguez-Padrón, E. Doustkhah, S. Ostovar, A. Franco, H. R. Shaterian and R. Luque, *Catal. Commun.*, 2019, **118**, 65–69.
96 S. Głowniak, B. Szczęśniak, J. Choma and M. Jaroniec, *Mater. Today*, 2021, DOI: 10.1016/j.mattod.2021.01.008.